HBRC Journal (2016) xxx, xxx–xxx

Housing and Building National Research Center

HBRC Journal

http://ees.elsevier.com/hbrcj

Effect of reinforcement ratios on shear behavior of concrete beams strengthened with CFRP sheets

Bashir H. Osman, Erjun Wu *, Bohai Ji, Suhaib S. Abdulhameed

College of Civil and Transportation Engineering, Hohai Univ., Nanjing 210098, China

Received 10 August 2015; revised 1 March 2016; accepted 2 April 2016

KEYWORDS

RC beams;
CFRP;
Reinforcement ratio;
Shear and flexural;
Cracks behavior;
ANSYS14

Abstract Carbon fiber reinforcement polymer (CFRP) sheets are the most commonly materials that are used to strengthen reinforced concrete members due to high strength-to-weight ratio, excellent mechanical strength, and good fatigue properties. In this research program seven reinforced concrete beams were tested under four points loading with different shear span-to-depth ratios $\left(\frac{a_v}{d}\right)$, longitudinal and vertical reinforcement ratios. A numerical analysis using ANSYS software program was done by modeling 27 reinforced concrete beams with and without CFRP sheets. The beam dimensions, concrete strength, strengthening configuration of the CFRP sheets (full wrapped, U shape, and side bonding), and FRP thickness were considered as the main parameters of the numerical analysis. A comparison between the finite element (FE) results and the ACI standard code demonstrated the validity of the computational models in capturing the structural response of FRP contribution with variation varied from (10–16)%, (12–20)% and (13–19)% for full wrapping, U-jacketing, and side bonding, respectively. The finite element models were able to accurately predict the load capacities for the simulated RC beams strengthened in shear with CFRP composites. The results obtained using ANSYS finite element are relatively identical to the experimental ones, showing reasonable agreement with variation not more than 5% in all the specimens.

Introduction

Reinforced concrete structures are widely used in civil engineering construction. Most of these structures may become deteriorated with time due to corrosion, freezing and thawing cycle, sulfate attack, and physical damage from impacts. Such deterioration may lead to inadequate flexural or shear strength of the concrete structure. The influence of reinforced concrete (RC) beam dimensions and effectiveness of stirrups in transferring shear across a diagonal crack were widely investigated by Tompos and Frosh [1], Bazant and Kim [2] and Godat et al.

* Corresponding author.
E-mail addresses: bashir00@yahoo.com (B.H. Osman), wwwerjun@hotmail.com (E. Wu), hhbhji@163.com (B. Ji), eng_suh@yahoo.com (S.S. Abdulhameed).

Peer review under responsibility of Housing and Building National Research Center.

ELSEVIER Production and hosting by Elsevier

http://dx.doi.org/10.1016/j.hbrcj.2016.04.002

[3]. Their results showed that the stirrups developed length can directly influence on shear strength while closed stirrups may have a significant influence on the strength contribution attributed to the stirrups. Moreover, the effect of reinforcement ratio in crack behaviors was carried out, and an algorithm with simplified formulas for estimating the relationship between the tension reinforcement and ductility of reinforced concrete beams was presented in Lee and Pan [4]. To evaluate the effective shear reinforcement pattern, a nonlinear analysis on RC beams with different shear reinforcement patterns using finite element analysis was conducted [5]. They also compared the existing variation in behaviors of reinforced concrete beam with and without shear reinforcement to that obtained from finite element simulation. Their results showed that all types of web reinforcements have almost similar effect for static loading condition.

Experimental and analytical studies regarding various configurations of FRP sheets to increase the strengthening effect of RC beams have been reported. For the length and anchorage length of CFRP, it has been recommended to use equations for the effective bond length from ACI repair manual [6]. However, experimental results have shown that the FRP length has no greater effect on structural behavior of RC beams when the FRP length is more than 60% of the span length of the beam [7,8]. The relationship between debonding and CFRP thickness is investigated experimentally [9,10]. They performed experiments to show the relationship between CFRP thickness and interfacial stress, and conclude that interfacial stress increases with the number of CFRP layers increased. Moreover, Brena and Marcri [11] investigated the effect of CFRP width on the structural behavior of RC beams.

The understanding of the shear resisting mechanisms in RC beams shear-strengthened by externally bonded fiber-reinforced polymer (FRP) sheets using finite element analysis was studied [12–14]. The presence of FRP reinforcements modifies the inclinations of cracks and struts, the concrete confinement stresses, and other parameters related to the shear response [15,16]. This directly produces an interaction between the concrete, internal steel, and FRP components of the shear strength.

The main contribution of this paper is to experimentally investigate the effect of reinforcement ratios and FRP strengthening on the shear behavior of reinforced concrete beams under four points loading. Moreover, the theoretical model of the ACI code for prediction of the behavior of the RC beam is experimentally validated. The beams were reinforced with different levels of steel reinforcement ratios and shear span-to-depth ratio $\left(\frac{a_v}{d}\right)$. The shear behavior was studied in terms of ultimate load, cracking load, crack patterns, and failure modes.

Experimental program

Details of tested beams

All reinforced concrete beams were constructed with a rectangular cross section of 100 mm wide, 300 mm high, and a total length of 1500 mm. One of these beams (beam RC0) was considered as a control beam, while beams (RC1–RC6) were reinforced with different reinforcement ratios. Beams (RC0 and RC1) were reinforced with 2Ø12 mm, Beam RC2 was reinforced with 4Ø12 mm, and Beams (RC3–RC6) were reinforced with 6Ø12 mm deformed bars at the tension face, while all the beams were reinforced with 2Ø10 mm deformed bars at the compression face. The Control beam (RC0) was left without shear reinforcement, while the remaining beams were provided with shear reinforcements consisting of Ø6 mm reinforcing bar stirrups at a center-to-center spacing of 150 mm, and 100 mm for beams (RC1–RC4) and (RC5 and RC6), respectively. The effective span-to-depth ratios $\left(\frac{a_v}{d}\right)$ were 1.5 for beams RC0–RC3 and RC6, while the $\frac{a_v}{d}$ was 2.0 for beams RC5 and RC6. The clear concrete cover to the reinforcement bars was 20 mm. Details of the tension, compression, and steel stirrups reinforcements are described in Fig. 1 and Table 1.

Material properties

Properties of the materials used in this research were obtained experimentally. The average concrete compressive strength was 33 MPa. The yield strength of the longitudinal and vertical

Table 1 Specimen details.

No	Specimen	$\frac{a_v}{d}$	Bott. steel	Top steel	Stirrup
1	RC0	1.5	2Ø12	2Ø10	–
2	RC1	1.5	2Ø12	2Ø10	Ø6@150
3	RC2	1.5	4Ø12	2Ø10	Ø6@150
4	RC3	1.5	6Ø12	2Ø10	Ø6@150
5	RC4	2.00	6Ø12	2Ø10	Ø6@150
6	RC5	2.00	6Ø12	2Ø10	Ø6@100
7	RC6	1.5	6Ø12	2Ø10	Ø6@100

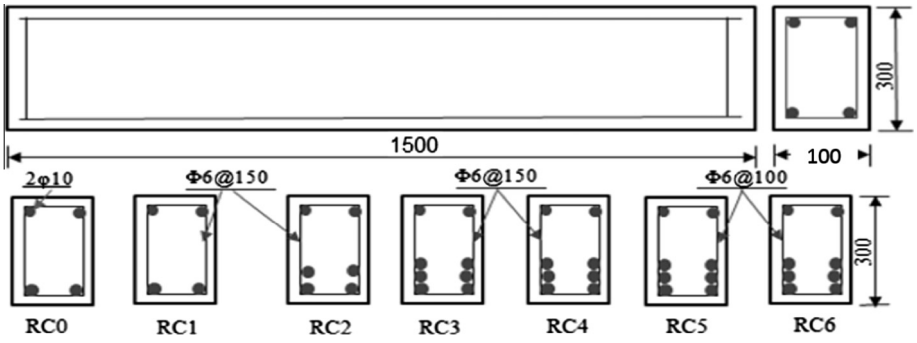

Figure 1 Geometry and cross sections of tested beam.

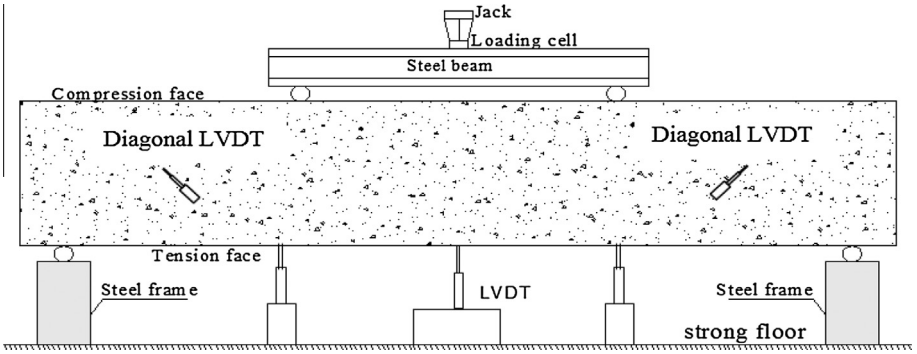

Figure 2 Test setup.

steel reinforcement was 360 MPa and 250 MPa, respectively, and the elastic modulus was 200 GPa.

Test setup

All the beams were tested under four points loading in the structural testing frame as shown in Fig. 2. Two heavy duty rollers were used to support the beams with a clear span equal to 1300 mm. These pin rollers provided bearing and frictionless rotational action during the test. Two additional rollers were used to apply loading on the beams. The distance between these two loads depends on the shear span-to-depth ratio of each beam ($1300 - a_v$). These two rollers were placed symmetrically about their centerline. The load was applied by using a universal testing machine. Prior to the actual tests, the specimens were initially loaded to a small fraction of the design ultimate load then unloaded so as to stabilize the beam and to prevent any possible twisting. The load was applied with increment of 10 kN using the load cell machine. The deflection values were recorded at each load increment. The load that causes the crack was recorded and its crack pattern was highlighted on the beam surface. The tested RC beams were instrumented with linear variable differential transducers (LVDTs) to monitor deflection and crack width during the test. The deflection during testing was measured using 100 mm LVDTs located under the two load points and at mid-span. Diagonal crack-width measurements were monitored and recorded using two 100 mm LVDTs, in the shear span as in Fig. 2.

Results and discussions

Experimental results

Crack patterns and failure mode

In the beam RC0, the first flexural cracks appeared in the constant moment region at 21.2 kN. By increasing the load, additional cracks generated and extended toward the shear span region.

Far ahead, large shear cracks with almost 45° from supports were created at load of 50.5 kN. Due to failure in the shear region, the beam was finally failed at load of 61 kN. In RC1, the first crack appeared in the mid-span at load of 23.1 kN. The diagonal shear cracks with a large slop outside the two loads and closer to them were created when more loads were applied. As the compressive concrete was breaking, and more cracks appeared parallel to that which was propagated toward the supports to the loading points, the beam was failed at 78 kN.

In spite of the difference in longitudinal reinforcement ratio of RC2, the failure mode and cracks pattern were similar to those of RC3. The first crack on these beams propagated in the supports region at 23.2 kN and 24 kN for RC2 and RC3 respectively. However, the number and extension of cracks seen in RC2 are more than that of RC3, particularly at the shear span zone. Finally, the concrete in shear region began to fail at 118.5 kN and 131.5 kN in RC2 and RC3 respectively when the cracks width increased. The load–displacement curves of the experimental and simulation results for the specimens RC0- RC3 are presented in Fig. 3.

The first crack on the beam RC4 was observed in the bending region at load of 20.02 kN, while the shear cracks with a very large slope outside the distance of two loads and close to the applied point loads appeared with the load increase up to 110.9 kN.

Then, the concrete of the compressive zone failed with combined shear and flexure failure mode at 125.2 kN as shown in Fig. 4. The failure mode and cracks in beam RC5 were similar to those of RC4 with some differences in the cracks number and width.

The first cracking load in RC5 started in the mid span at 22.3 kN. After increasing load, cracks width was increased rapidly, while the beam had failure in shear followed by flexure failure at 135 kN with maximum deflection of 2.35 mm as shown in Fig. 5.

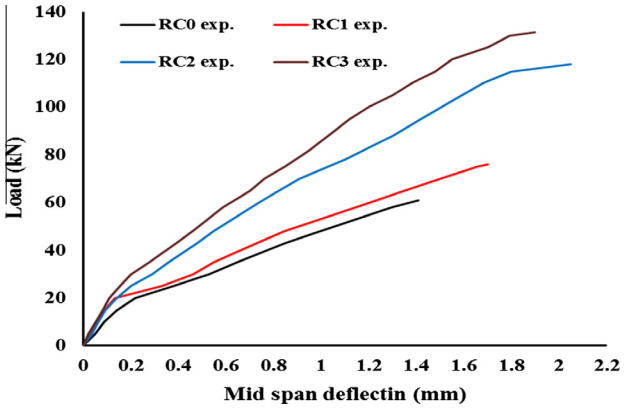

Figure 3 Effect of longitudinal reinforcement on ultimate load.

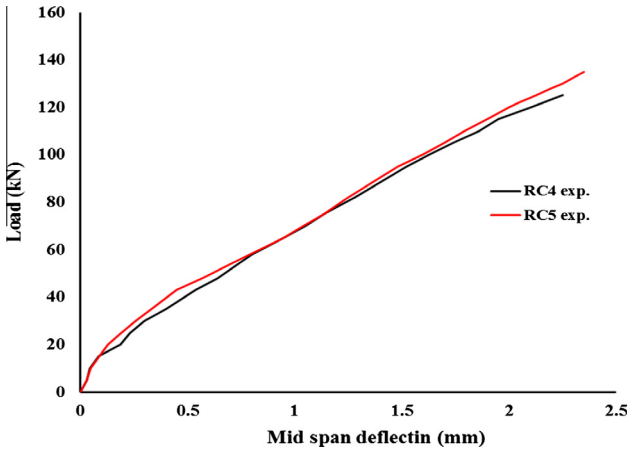

Figure 4 Effect of transverse reinforcement on ultimate load and deflection.

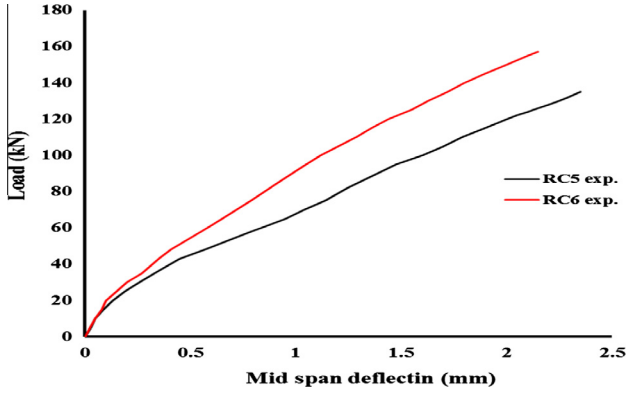

Figure 5 Effect of span-to-depth ratio on ultimate load.

In beam RC6, it can be observed that the cracks were considerably smaller than that of the other beams while the crack shape is similar to that of RC5, however, at earlier loading value of 22.15 kN. After increasing load, the concrete in the compressive area started to fail and the failure crack initiated at the support point and propagated toward the loading point at 157.03 kN. The value of failure loads in this beam was higher than all test beams.

From the above observations, the cracks width of specimens indicates that the use of longitudinal reinforcement ratio has a significant effect on the crack width and space at every load stages. It is obvious that wider cracks were considerably measured in specimens with lower shear reinforcement than that with higher reinforcement ratio values. Fig. 6 shows the sample of the load versus the crack width of four tested beams. The beams with additional tension reinforcement displayed better cracking control than that of control beam by decreasing the cracks width and increasing the spacing between the cracks. The cracks patterns of tested beam are illustrated in Fig. 7.

Numerical modeling

A finite element (FE) analysis using ANSYS [17] computer program was used to analysis the reinforced concrete (RC)

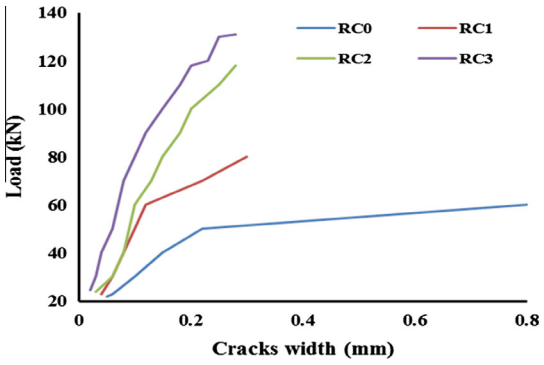

Figure 6 Sample of load versus the crack width of four tested beams.

beams. The numerical simulation was divided into two groups. The first group consisted on the calibration of the numerical models with the experimental results, while the second group was investigated the effect of beam depth, concrete strength, CFRP sheet configuration, and CFRP sheet thickness on the behavior of reinforced concrete beams strengthened with CFRP sheets.

SOLID65 element, was used to model the concrete, and this element is capable of cracking in tension and crushing in compression. The element is defined by eight nodes having three degrees of freedom at each node: translations of the nodes in x, y, and z-directions.

An eight-node solid element, solid 45, was used to simulate the steel plates in the supports and the loading points. The element is defined with eight nodes having three degrees of freedom at each node translation in the nodal x-, y-, and z-directions.

A link 8 element was used to model steel reinforcement. This element is a 3D spar element and it has two nodes with three degrees of freedom in each node The finite element model for the rebar was assumed to be a bilinear isotropic, elastic-perfectly plastic material, and identical in tension and compression.

A layered solid element, Solid 46, was used to model the FRP sheet. The element allows for different material layers with different orientations and orthotropic material properties in each layer. The element has three degrees of freedom at each node. Eqs. (1) and (2) show the relationship between vxy and vyx:

$$1 - v_{xy}^2\left(\frac{E_y}{E_x}\right) - v_{yz}^2\left(\frac{E_z}{E_y}\right) - v_{xz}^2\left(\frac{E_z}{E_x}\right) - 2v_{xy}v_{yz}v_{xz}\left(\frac{E_z}{E_x}\right) = \text{positive} \quad (1)$$

$$G_{xy} = G_{xz} = \frac{E_x E_y}{E_x + E_y + 2v_{xy}E_x}, \quad G_{yz} = \frac{E_z \text{ or } E_y}{2(1+v_{yz})} \quad \text{and} \quad v_{yx} = \frac{E_y}{E_x}v_{xy} \quad (2)$$

In the present study, the linear elastic properties of FRP composites are assumed. Poisson's ratios of: $vxy = vxz = 0.22$ and $vyz = 0.30$, which are widely used in previously published literature on this subject, are adopted. The contact between FRP and concrete is modeled by contact elements TARGE170 and CONTA174 (ANSYS 14) [15,18]. In studying the contact

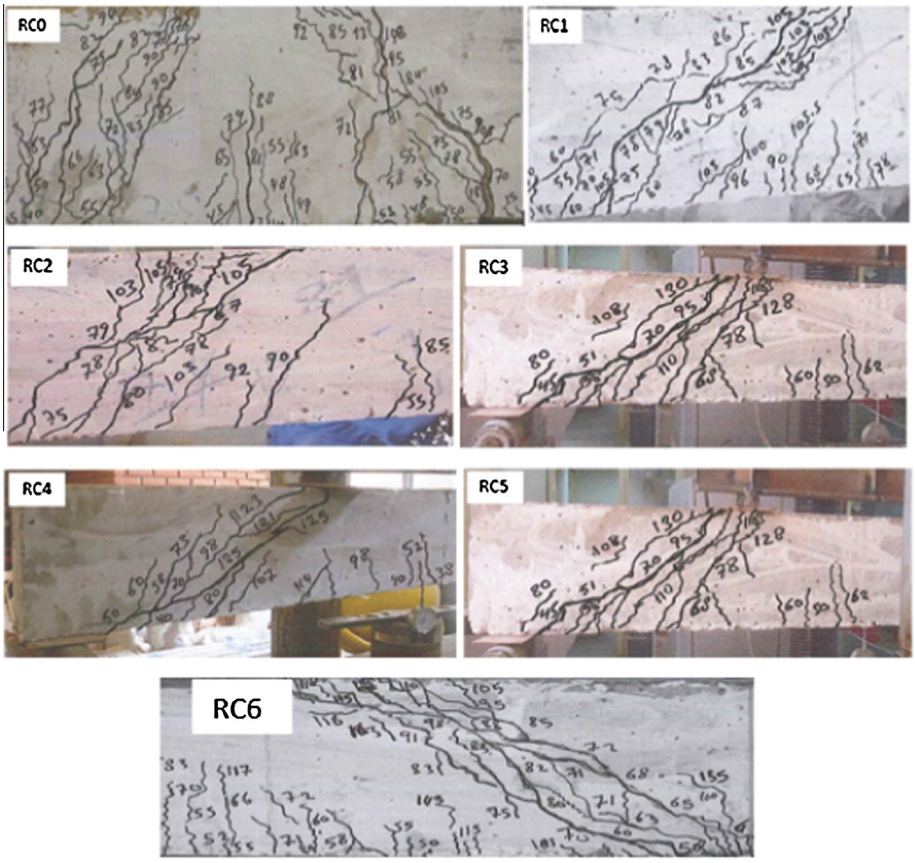

Figure 7 Crack patterns of tested beams.

between two bodies, the surface of one body is conventionally taken as a contact surface (e.g. FRP) and the surface of the other body as a target surface (e.g. concrete). The "contact-target" pair concept has been widely used in finite element simulations. As used in this study, the FRP was considered as the contact surface which is associated with the deformable body; the concrete was considered as the target surface which must be the rigid surface.

Verification study

The FE models were calibrated with the experimental results. The goal of this comparison is to verify the validity of the model and analysis. As shown in Fig. 8(a–c) it is evident that there is a very good correlation between the numerical and experimental load–deflection curves at all loading stages. The finite element models were able to accurately predict the load capacities for the simulated RC beams. This confirms the validity of the developed FE models and reliability of the FE simulation.

Table 2 gives the numerical and experimental failure load, failure mode, and deflection for all tested beams.

The ANSYS proposed model results showed acceptable agreement with the experimental results with variation ranged from (3–9)%, (2–5)% and (1.5–3.5)% for ultimate load, cracking load and deflection respectively, as in Table 2. However, the difference increased to 19% and (10–40)% for ultimate load and deflection respectively compared to ACI approach.

Parametric study for prediction of shear capacity of RC beams using FE simulation

A parametric study was carried out to evaluate the effects of those parameters on the shear capacity. The parameters included the FRP thickness, the concrete strength, and the effective height of the beam. Meanwhile, 27 specimens were analyzed numerically by considering the effect of beam depth, concrete strength, strengthening configuration (full wrapped, U, and side bonding), and FRP thickness and the results were compared with the ACI codes. The designed shear capacity Vn of the FRP-strengthened RC beam was calculated from Eq. (3):

$$Vn = Vc + Vs + Vf \tag{3}$$

where Vc is contribution of concrete; Vs is contribution of the steel stirrups; and Vf is contribution of the FRP. Vc and Vs are calculated according to the provisions in existing RC design codes (ACI 318 2011). The main differences among the various existing models lie in the evaluation of the FRP contribution Vf.

The model proposed by ACI 440 [6] is applicable to RC beams externally-strengthened with FRP reinforcement and can be calculated by

$$Vf = \frac{nW_f t_f E_f \varepsilon_{fe} d_f}{s_f} \tag{4}$$

$\varepsilon fe = 0.004 \leqslant 0.75\varepsilon fu$ for completely wrapped or $\varepsilon fe = K\nu\varepsilon fu \leqslant 0.004$ for two or three sides laminated.

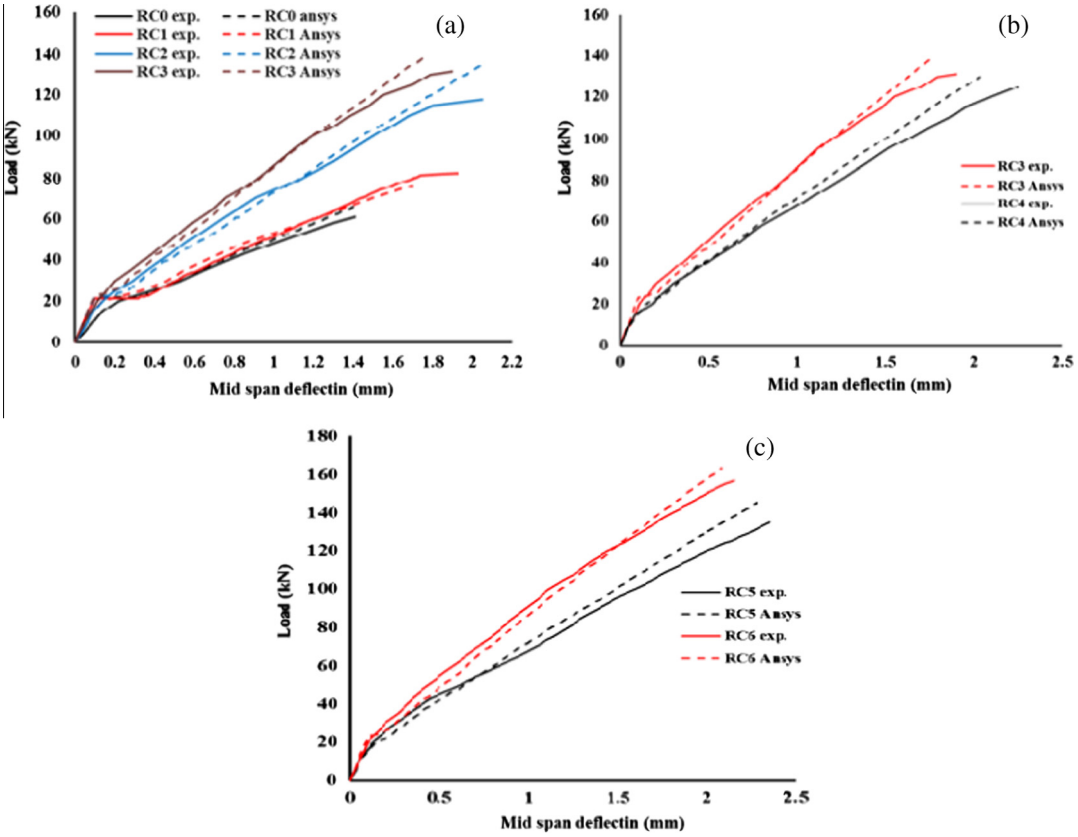

Figure 8 Load deflection curve for FE verification.

Table 2 Summary of experimental, ANSYS finite element and ACI results with failure mode.

Beam No	$\frac{a_v}{d}$	Ultimate load (P)			Ultimate deflection (mm)			Cracking load (Pcr)		$P_{exp.}/P_{ANSYS}$	$P_{exp.}/P_{ACI}$	Mode of failure
		$P_{exp.}$ (kN)	P_{ANSYS} (kN)	P_{ACI} (ACI)	$Def_{exp.}$ (mm)	Def_{ANSYS} (mm)	Def_{ACI} (mm)	$Pcr_{exp.}$ (kN)	Pcr_{ANSYS} (kN)			
RC0	1.5	61	65.5	58.30	1.41	1.39	0.83	21.2	21.74	0.93	1.04	S* & F
RC1	1.5	78	84.5	103.02	1.85	1.93	1.40	23	23.54	0.92	0.76	S*
RC2	1.5	118	135	112.44	2.05	1.98	1.53	23.2	24.01	0.87	1.04	S*
RC3	1.5	131.5	140.6	119.10	1.90	1.77	1.62	24	24.5	0.94	1.10	S*
RC4	2	125.1	130.4	111.28	2.25	2.04	1.51	20	20.3	0.96	1.12	S* & F
RC5	2	135	145.03	133.60	2.35	2.28	1.82	22.3	23	0.93	1.01	S* & F
RC6	1.5	157	163.1	139.50	2.15	2.09	1.90	22.2	23.5	0.96	1.13	S*

* S = Shear, F = Flexure.

$$Kv = \frac{k1k2Le}{11,900\varepsilon fu} \leqslant 0.75, \quad Le = \frac{23,300}{(tfEf)^{0.58}}; \quad k1 = \left(\frac{fc}{27}\right)^{\frac{2}{3}} \qquad (5)$$

$$k2 = \frac{(df - Le)}{df} \text{ for U-jacketing, } k2$$

$$= \frac{(df - 2Le)}{df} \text{ for two sides laminated}$$

where df = depth of FRP shear reinforcement, Ef = tensile modulus of elasticity of FRP, $k1$ = modification factor applied to kv to account for the concrete strength, $k2$ = modification factor applied to kv to account for the wrapping scheme, Le = active bond length of FRP laminate, n = number of plies of FRP reinforcement, wf = width of the FRP reinforcing plies, εfe = effective strain level in FRP reinforcement; strain level attained at section failure, εfu = design rupture strain of FRP reinforcement, sf = spacing FRP shear reinforcing, and fc = compressive stress in concrete.

Influence of the FRP thickness

The thickness (t_f) of FRP is the main factor that directly affects the strength and the stiffness of the strengthening material. The variations of the predicted FRP contribution versus FRP thickness for design guidelines are shown in Fig. 9.

Please cite this article in press as: B.H. Osman et al., Effect of reinforcement ratios on shear behavior of concrete beams strengthened with CFRP sheets, HBRC Journal (2016), http://dx.doi.org/10.1016/j.hbrcj.2016.04.002

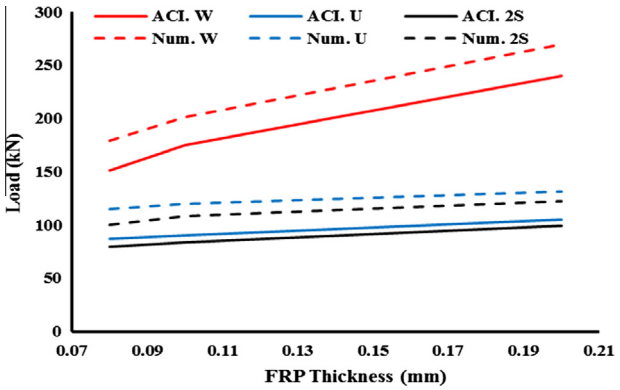

Figure 9 Influence of the FRP thickness by the existing models and the FE simulations.

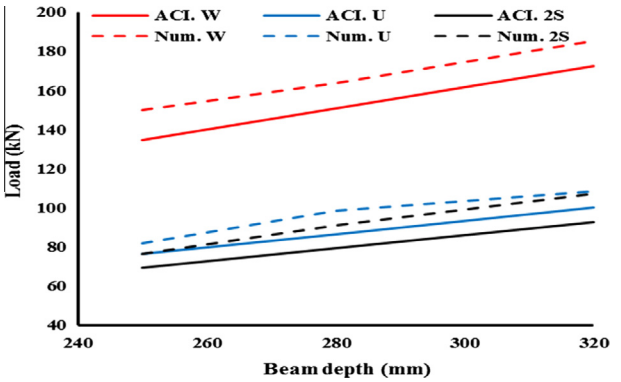

Figure 11 Influence of the beam depth by the existing models and the FE simulations.

The predicted results were in good agreement with the ACI results with variation not more than 16%, 20% and 19% for full warp, U, and side bond, respectively.

Influence of concrete strength

The concrete strength is also an important factor that directly affects the strength and the stiffness of the strengthening material. The variations of the predicted FRP contributions versus concrete strength for design guidelines are shown in Fig. 10. A comparison between the FE results and the ACI standard code demonstrated the validity of the computational models in capturing the structural response with variation not more than 11%, 18% and 15% for full warp, U, and side bond, respectively.

Influence of the beam depth

It is adopted that the shear capacity of the completely-wrapped beam is affected by the increase in the height of the FRP sheet more than U and side bonds as shown in Fig. 11. The predicted results from FE were in good agreement with the ACI code results with variation not more than 10%, 12% and 13% for full warp, U, and side bond, respectively.

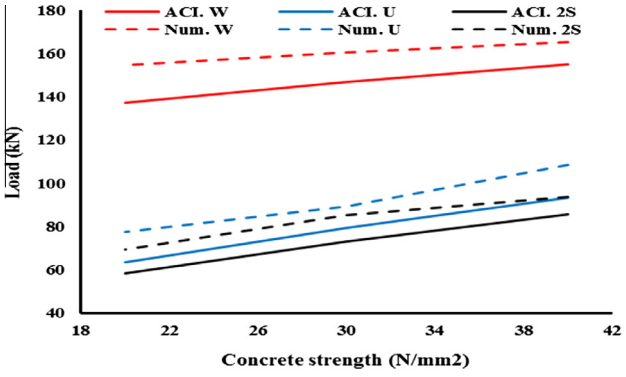

Figure 10 Influence of the concrete strength as predicted by the existing models and the FE simulations.

Conclusion

In this paper, seven reinforced concrete (RC) beams under four-point loading with different shear span-to-depth ratios, longitudinal and vertical reinforcement ratios were experimentally investigated. The FE simulation approach was adopted to predict the contribution of side bonding, U-jacketing and full wrapping FRP to the shear capacity of the RC beams. Parametric studies were conducted to evaluate the importance of different parameters that affect the shear capacity of the RC beam. It is obvious that as the longitudinal reinforcement ratio is increased, there is a small increase in the concrete shear strength, owing to the low contribution of longitudinal steel in the shear capacity of the beams loaded on shear zone. Moreover, the stirrups reinforcement ratio has a great influence on the shear strength and cracks depth than other parameters. The primary shear crack inclination affects the shear strength contribution of the shear reinforcement. Furthermore, as the shear crack angle determines the number of stirrups intersected by the crack, the stirrup directly affects the shear strength. It has been further shown that the low reinforcement ratios directly reduce the shear strengths of the specimens and increase the crack widths. All specimens show that the effect of the reinforcement ratio on shear strength and deflection was considerably greater than that predicted by ACI equations particularly in deflection. The results obtained using ANSYS finite element were relatively identical to the experimental ones, with variation not more than 5% in all the specimens.

A comparison between the FE results and the ACI standard code demonstrated the validity of the computational models in capturing the structural response of FRP contribution with variation varied from (10–16)%, (12–20)% and (13–19)% for full wrapping, U-jacketing and side bonding, respectively. The finite element models were able to accurately predict the load capacities for the simulated RC beams strengthened in shear with FRP composites. This confirms the validity of the developed FE models and reliability of the ANSYS FE simulation.

Conflict of interest

Author states that there is no conflict of interest.

References

[1] Eric J. Tompos, Robert J. Frosh, Influence of beam size, longitudinal reinforcement, and stirrup effectiveness on concrete shear strength, ACI Struct. J. 99 (2002) 559–567.
[2] Zdenek P. Bazant, Jin-Keun Kim, Size effect in shear failure of longitudinally reinforced beams, ACI J. 81 (1984) 456–468.
[3] A. Godat, Z. Qu, X.Z. Lu, P. Labossière, L.P. Ye, K.W. Neale, M. ASCE, Size effects for reinforced concrete beams strengthened in shear with CFRP strips, J. Compos. Constr. 14 (2010) 260–271.
[4] Tai-Kuang Lee, Austin D.E. Pan, Estimating the relationship between tension reinforcement and ductility of reinforced concrete beam sections, Eng. Struct. 25 (2003) 1057–1067.
[5] I. Saifullah, M.A. Hossain, S.M.K. Uddin, M.R.A. Khan, M.A. Amin, Nonlinear analysis of RC beam for different shear reinforcement patterns by finite element analysis, Int. J. Civ. Environ. Eng. (IJCEE-IJENS) 11 (2011) 63–74.
[6] ACI Committee 440, Guide for the Design and Construction of Externally Bonded FRP Systems for Strengthening Concrete Structures (ACI 440.2R-02), American Concrete Institute, Farmington Hills, Mich., 2008.
[7] Bo Mangi, B. Abdeljelil̈n, S.W. Bae, Effect of bond length of FRP sheets externally bonded to concrete, Int. J. Concr. Struct. Mater. 3 (2009) 127–131.
[8] M.M.A. Kadhim, Effect of CFRP sheets length on the behavior of HSC continuous beam, J. Thermoplast Compos. Mater. 25 (2012) 33–44.
[9] C. Leung, CFRP debonding from a concrete substrate: some recent findings against conventional belief, Cem. Concr. Compos. 28 (2006) 742–748.
[10] M. Maalej, K.S. Leong, Effect of beam size and FRP thickness on interfacial shear stress concentration and failure mode of FRP- strengthened beams, Compos. Sci. Technol. 65 (2005) 1148–1158.
[11] S.F. Brena, B.M. Marcri, Effect of carbon fiber reinforced polymer laminate configuration on the behavior of strengthened reinforced concrete beams, J. Compos. Constr. 8 (2004) 229–240.
[12] Denise Ferreira, Eva Oller, Antonio Marí, M. ASCE, Jesús Bairán, Numerical analysis of shear critical RC beams strengthened in shear with FRP sheets, J. Compos. Constr. 17 (2013) 1–11.
[13] A. Godat, K.W. Neale, P. Labossière, Numerical modeling of FRP shear-strengthened reinforced concrete beams, J. Compos. Constr. 6 (640) (2007) 640–649.
[14] R. Wong, F.J. Vecchio, Towards modelling of reinforced concrete members with externally bonded fiber-reinforced polymer (FRP) composites, ACI Struct. J. 100 (2003) 47–55.
[15] D. Kachlakev, D. McCurry, Simulated full scale testing of reinforced concrete beams strengthened with FRP composites: Experimental results and design model verification, Final Rep. FHWA-OR-RD-00-19, Oregon Dept. of Transportation and U. S. Dept. of Transportation Federal Highway Administration, Salem, OR, 2000.
[16] Kachlakev Damian, Miller Thomas, Finite Element Modeling of Reinforced Concrete Structures Strengthened with FRP Laminates, Civil, Construction and Environmental Engineering Department, Oregon State University, Corvallis, OR 97331, 2001.
[17] ANSYS Version 14 Houston [Computer software], Swanson Analysis Systems, Texas.
[18] Suhaib S. Abdulhameed, Erjun Wu, Bohai Ji, Mechanical prestressing system for strengthening reinforced concrete members with prestressed carbon-fiber-reinforced polymer sheets, J. Compos. Constr. 29 (3) (2013) 04014081.

Please cite this article in press as: B.H. Osman et al., Effect of reinforcement ratios on shear behavior of concrete beams strengthened with CFRP sheets, HBRC Journal (2016), http://dx.doi.org/10.1016/j.hbrcj.2016.04.002